

RESEARCH ARTICLE

NADPH oxidase 1 is a novel pharmacological target for the development of an antiplatelet drug without bleeding side effects

Dina Vara¹ | Anuradha Tarafdar¹ | Meral Celikag¹ | Daniela Patinha¹ |
 Christina E. Gulacsy² | Ellie Hounslea² | Zach Warren¹ | Barbara Ferreira¹ |
 Maarten P. Koeners¹ | Lorenzo Caggiano² | Giordano Pula³

¹Institute of Biomedical and Clinical Science, University of Exeter Medical School, Exeter, UK

²Department of Pharmacy and Pharmacology, University of Bath, Bath, UK

³Institute of Clinical Chemistry and Laboratory Medicine, University Medical Centre Hamburg-Eppendorf, Hamburg, Germany

Giordano Pula, Institute of Clinical Chemistry and Laboratory Medicine, University Medical Centre Hamburg-Eppendorf, Hamburg, Germany.
 Email: g.pula@uke.de

Funding information

British Heart Foundation (BHF), Grant/Award Number: FS/14/2/30630, PG/15/40/31522 and PG/15/68/31717; Alzheimer's Research UK (ARUK), Grant/Award Number: ARUK-PG2017A-3; British Heart Foundation (BHF)

Abstract

Growing evidence supports a central role of NADPH oxidases (NOXs) in the regulation of platelets, which are circulating cells involved in both hemostasis and thrombosis. Here, the use of *Nox1*^{-/-} and *Nox1*^{+/+} mice as experimental models of human responses demonstrated a critical role of NOX1 in collagen-dependent platelet activation and pathological arterial thrombosis, as tested in vivo by carotid occlusion assays. In contrast, NOX1 does not affect platelet responses to thrombin and normal hemostasis, as assayed in tail bleeding experiments. Therefore, as NOX1 inhibitors are likely to have antiplatelet effects without associated bleeding risks, the NOX1-selective inhibitor 2-acetylphenothiazine (2APT) and a series of its derivatives generated to increase inhibitory potency and drug bioavailability were tested. Among the 2APT derivatives, 1-(10*H*-phenothiazin-2-yl)vinyl *tert*-butyl carbonate (2APT-D6) was selected for its high potency. Both 2APT and 2APT-D6 inhibited collagen-dependent platelet aggregation, adhesion, thrombus formation, superoxide anion generation, and surface activation marker expression, while responses to thrombin or adhesion to fibrinogen were not affected. In vivo administration of 2APT or 2APT-D6 led to the inhibition of mouse platelet aggregation, oxygen radical output, and thrombus formation, and carotid occlusion, while tail hemostasis was unaffected. Differently to in vitro experiments, 2APT-D6 and 2APT displayed similar potency in vivo. In summary, NOX1 inhibition with 2APT or its derivative 2APT-D6 is a viable strategy to control collagen-induced platelet activation and reduce thrombosis without deleterious effects on hemostasis. These compounds should, therefore, be considered for the development of novel antiplatelet drugs to fight cardiovascular diseases in humans.

Abbreviations: 2APT, 2-acetylphenothiazine; ANOVA, analysis of variance; CAD, coronary artery disease; CGD, granulomatous disease; CMH, 1-hydroxy-3-methoxycarbonyl-2,2,5,5-tetramethylpyrrolidine; DETC, diethyldithiocarbamate; DiOC6, 3,3'-Dihexyloxycarbocyanine Iodide; DMSO, dimethyl sulfoxide; EPR, electron paramagnetic resonance; FeCl₃, ferric chloride; FITC, fluorescein isothiocyanate; NOXs, NADPH oxidases; PAD, peripheral artery disease; PE, phycoerythrin; PGE1, prostaglandin E1; PPACK, D-Phenylalanyl-prolyl-arginyl Chloromethyl Ketone; PRP, platelet-rich plasma; ROS, reactive oxygen species; TRITC, tetramethylrhodamine.

Lorenzo Caggiano and Giordano Pula contributed equally to this study.

This is an open access article under the terms of the Creative Commons Attribution License, which permits use, distribution and reproduction in any medium, provided the original work is properly cited.

© 2020 The Authors. *The FASEB Journal* published by Wiley Periodicals LLC on behalf of Federation of American Societies for Experimental Biology

KEYWORDS

free radical, hemostasis, NADPH oxidase, oxidative stress, platelet, redox, thrombosis

1 | INTRODUCTION

Platelets are anucleated cells released in the bloodstream by their progenitors residing in the bone marrow, the megakaryocytes. Platelets are responsible for the initiation of hemostasis, which is the interruption of bleeding upon vascular damage. Hemostasis consists of primary hemostasis, which is the activation, adhesion, and accumulation of platelets at the site of injury in the form of thrombi, and secondary hemostasis, which is the activation of the coagulation cascade leading to the deposition of fibrin within thrombi to form blood clots. Primary and secondary hemostasis are tightly connected, with platelet activation during primary hemostasis facilitating the initiation of coagulation, and secondary hemostasis driving platelet activation via the generation of thrombin as one of the main products of the coagulation cascade. The distinction between primary and secondary hemostasis was made to help our understanding of this phenomenon, but has no temporal or spatial relevance, as these two events occur within the same microenvironment with overlapping kinetics. The unwanted blood vessel occlusion due to either platelet or coagulation activation is known as thrombosis. Thrombosis is responsible for important vascular diseases such as stroke, coronary artery disease (CAD), and peripheral artery disease (PAD). Antithrombotics can be divided into antiplatelet or anticoagulant drugs, depending on whether they target primary or secondary hemostasis, respectively. Oxidative stress is the dysregulated generation of reactive oxygen species (ROS) and has been shown to cause platelet hyperactivity leading to thrombosis.¹⁻⁴ NADPH oxidases (NOXs) are important sources of ROS in platelets⁵⁻⁷ and their function promotes platelet activation.^{8,9} NOXs are a family of multimeric plasma membrane complexes generating the majority of non-mitochondrial ROS in mammalian cells. Each complex consists of a catalytic subunit and a number of regulatory subunits responsible for the maturation, stabilization, haem incorporation, and translocation to the cell membrane of the enzymatically functional complex. All NOX family members act as catalysts for the transfer of electrons from NADPH to molecular oxygen to form ROS. NOX1, NOX2, NOX3, and NOX5 generate superoxide anion, while NOX4, DUOX1, and DUOX2 release hydrogen peroxide. Although platelet NOX2 has been investigated,⁴ the expression of NOX1 in human platelets has only been described relatively recently.¹⁰ Despite the established importance of NOXs in the molecular mechanisms leading to platelet activation,^{8,9,11} the exact

role of different NOX isoenzymes, and the molecular mechanism linking NOX activity to platelet regulation remains uncertain.^{9,12-14} Nonetheless, a convincing amount of evidence suggests that the enzymatic activity of NOXs plays a significant role in promoting platelet responses.¹⁵ Therefore, several pharmacological tools for the inhibition of NOXs that have been recently developed and described may have important platelet modulatory effects.^{10,16-21} If that is confirmed, NOX inhibitors may become novel antiplatelet drugs to add to existing cardiovascular treatments. They may be particularly useful for vascular complications caused by platelet hyperactivity, as observed in diabetes, metabolic syndrome, hypertension, and atherosclerosis.^{1,5,6,22} Interestingly, the efficacy of NOX inhibition in patients displaying resistance to traditional antiplatelet drugs has been described,²³ suggesting that targeting NOXs may become a valid alternative to fight thrombosis.¹¹

The work from our and other laboratories highlighted the central role of NOX1 in the signal transduction of collagen-dependent platelet activation.^{13,24} Recently, we utilized selective agonists and a novel electron paramagnetic resonance-based technique to show that the signaling of the collagen receptor GPVI requires NOX1.¹⁴ These results are paralleled by a recent study showing that NOX2 is dispensable for GPVI-dependent activation of platelets *ex vivo* and the carotid thrombosis induced by photochemical injury *in vivo*.¹² This recent evidence is in contrast with previous studies indicating NOX2 as critical for the activation of platelets by collagen and for the development of thrombosis *in vivo*.⁹ Although differences in the methodologies may partly explain this discrepancy (eg, ferric chloride vs photochemical vascular injury *in vivo*), the exact roles of different NOX family members in the redox-dependent regulation of platelets remain to be fully explained. Other aspects that remain to be elucidated are the mechanisms of activation of NOXs in platelets and the downstream signaling that they activate. Currently, a role for the small GTPase Rac1 has been proposed for the activation of NOXs in platelets,^{25,26} while the most likely mechanism of signal transduction that they trigger involves the oxidative inactivation of the protein phosphatase SHP2 resulting in the potentiation of the protein kinase cascade activated by GPVI in response to collagen.^{27,28}

In this study, we aimed to test the effect of the NOX1 inhibitor 2-acetylphenothiazine (2APT) and a series of its derivatives for their effect on platelets *in vitro* and for their ability to be absorbed via oral administration in mice and

affect platelet responses *ex vivo* or hemostasis/thrombosis responses *in vivo*. 2APT derivatives were designed to resolve the two main weaknesses of 2APT: (1) small concentration window at which the drug is selective for NOX1 (ie, no effect on NOX1 below 200nM and inhibition of other NOXs above 3 μ M)²¹; (2) undesirable hydrophobic profile.

2 | METHODS

2.1 | 2APT derivative synthesis

Detailed synthesis and purity control procedures are described in the Methods Supplement, while compound structures are described in Figure 1.

2.2 | Mouse maintenance, murine blood collection, and platelet preparation

Previously described *Nox1*^{-/-29} and *Nox2*^{-/-30} mice were utilized for this study. Mouse maintenance was performed according to the local ethical approval (University of Exeter) and Home Office licensing for Scientific Procedures (PPL30/3348). Although only 12-week-old female mice were utilized for experiments throughout this manuscript, initial characterization experiments showed that for all the mouse strains used in this project, platelet aggregation responses in male and female animals are comparable (ie, no sexual difference). For washed platelets, sodium citrate was used as an anticoagulant (0.5% w/v). Platelet-rich plasma (PRP) was separated from whole blood by centrifugation (180 \times g, 15 minutes) and platelets were separated from PRP by a second centrifugation step (600 \times g, 10 minutes) in the presence of prostaglandin E1 (PGE1, 40 ng/mL) and indomethacin (10 μ M). Platelets were resuspended in modified Tyrode's buffer at a density of 2 \times 10⁸ platelets/mL throughout the study. For whole blood analyses (eg, thrombus formation), heparin and D-Phenylalanyl-prolyl-arginyl Chloromethyl Ketone (PPACK)-anticoagulated whole blood were used (5 unit/mL and 25 μ M, respectively).

2.3 | Platelet aggregation by turbidimetry

Platelets resuspended in modified Tyrode's buffer at a density of 2 \times 10⁸ platelets/mL were stimulated using a Chrono-Log 490 4 + 4 aggregometer (Havertown, US). Aggregation was induced with 0.1 unit/mL of human thrombin or 3 μ g/mL of Horm collagen. Absorbance was measured for 10 minutes and expressed as % change in absorbance.

2.4 | Carotid occlusion model

The procedure has been performed as described previously described.^{31,32} Briefly, anesthesia was induced with 4% isoflurane and maintained at 1.5%-2% isoflurane. The carotid artery was surgically exposed and fitted with a miniature transonic flow probe (Transonic Systems Inc TS420, USA). The probe was linked to a CED Micro1401 acquisition unit (Cambridge Electronic Design Limited, UK) via a flowmeter (Transonic Systems Inc, USA). Ferric chloride (FeCl₃, 10% w/v) was applied topically to the exposed artery via a piece of filter paper (1 \times 1.5 mm) to induce thrombus formation. After 5 minutes, the filter paper was removed, while blood flow was continuously recorded until cessation (ie, occlusion) or alternatively up to 40 minutes in occlusion-free mice. Data were acquired using Spike2 (Cambridge Electronic Design Limited, UK) software. Time to occlusion after the FeCl₃ challenge was analyzed and utilized as a measure of susceptibility to thrombosis. Hematoxylin staining of explanted carotid sections after ferric chloride treatment was used to confirm occlusion.

2.5 | Tail tip transection assay

Mice were anesthetized by the inhalation of 4% isoflurane and continuously maintained at 1.5% isoflurane. The animals were placed in the prone position and a 3-mm segment of the tail was amputated with a scalpel. The tail was immediately immersed in pre-warmed isotonic saline at 37°C. The bleeding time was measured manually.

2.6 | Electron paramagnetic resonance (EPR)

As described in our previous study,¹⁴ prior to adding stimuli, 200 μ M 1-hydroxy-3-methoxycarbonyl-2,2,5,5-tetramethylpyrrolidine (CMH), 5 μ M diethyldithiocarbamate (DETC), and 25 μ M deferoxamine were added to platelets (density adjusted to 2 \times 10⁸ platelets/mL) with continuous stirring. After 1 minute, stimuli were delivered and 10 minutes later 50 μ L of platelet-free supernatant was collected and read using an E-scan (Noxygen, Germany). EPR spectra were recorded using the following EPR settings: center field 3490 G, field sweep 60 G, modulation amplitude 2 G, sweep time 10 seconds, number of scans 10, microwave frequency 9.39 GHz. A calibration curve was obtained from standard CM[•] diluted to concentrations of 0, 0.3, 1, 3, 10, and 30 μ M and utilized to estimate the CM[•] concentration in the samples as described in Figure S1. The CMH oxidation rate was obtained using the following formula: CMH oxidation rate = [CM[•]] \times Volume / (Platelet density \times Volume \times Time).

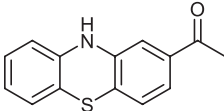
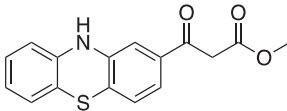
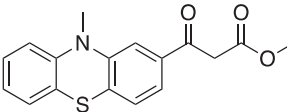
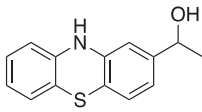
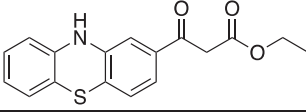
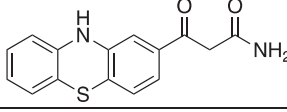
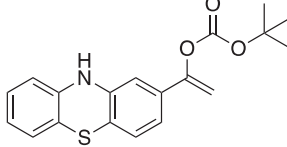
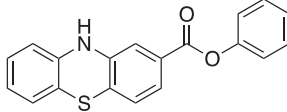
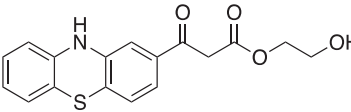
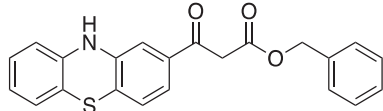
	Molecular Weight (g/mol)	cLogP
2APT 	241.31	3.93
2APT-D1 	299.34	3.70
2APT-D2 	313.37	3.88
2APT-D3 	243.32	3.18
2APT-D4 	313.37	4.23
2APT-D5 	284.33	2.58
2APT-D6 	341.43	4.39
2APT-D7 	319.38	5.97
2APT-D8 	329.37	3.04
2APT-D9 	375.44	5.41

FIGURE 1 2APT derivative structures and calculated partition coefficients (cLogP). The cLogP values were calculated using the ChemDraw software package from Alfasoft™ (Goteborg, Sweden)

2.7 | Human blood collection and platelet preparation

Procedures utilizing human blood conform to the principles outlined in the Declaration of Helsinki. Volunteers were

male and female between ages 25 and 65, with no diagnosis of cardiovascular disease, diabetes or cancer. Volunteers on antiplatelet, anticoagulant, and anti-inflammatory drugs were excluded from the study. Human blood was drawn from the median cubital vein venepuncture following the

Royal Devon and Exeter NHS Foundation Trust Code of Ethics and Research Conduct and under National Research Ethics Service South West—Central Bristol approval (Rec. n. 14/SW/1089). Informed written consent was given prior to the inclusion of participants in the study. Sodium citrate was used as an anticoagulant (0.5% w/v). Platelet-rich plasma (PRP) was separated from whole blood by centrifugation (250× g, 17 minutes) and platelets were separated from PRP by a second centrifugation step (500× g, 10 minutes) in the presence of prostaglandin E1 (PGE1, 40 ng/mL) and indomethacin (10 μM). For whole blood analyses (eg, thrombus formation), heparin- and PPACK-anticoagulated whole blood was used.

2.8 | Platelet static adhesion

Platelets at a density of 2×10^7 platelets/mL were treated with NOX inhibitors for 10 minutes and then seeded on collagen- or fibrinogen-coated coverslips for 30 minutes at 37°C. After the removal of non-adhering cells, platelets were fixed with 4% paraformaldehyde for 10 minutes. After permeabilization with 0.1% Triton X/PBS, 10 μM tetramethylrhodamine (TRITC)-conjugated phalloidin was utilized to stain the actin cytoskeleton. Quantification of platelet adhesion was obtained by LED fluorescence microscopy (EVOS Fl) and image analysis using ImageJ 1.47v (Wayne Rasband, National Institute of Health, USA).

2.9 | Thrombus formation under physiological flow assay

In order to test collagen-dependent platelet activation and thrombus formation in physiological flow conditions, a flow assay was performed in anticoagulated blood as previously described.³³ Human or mouse blood was anticoagulated with 5 u/mL of heparin and 40 μM PPACK and labeled with 1 μM 3,3'-Dihexyloxycarbocyanine Iodide (DiOC6) for 10 minutes. Ibidi Vena8 Fluoro + flow microchips and a Cellix Exigo pump were utilized to analyze thrombus formation in whole blood underflow. Microchips were coated with Horm collagen (0.1 μg/mL). Thrombus formation was visualized by fluorescence microscopy at a shear rate of 1000 sec⁻¹. Surface coverage was analyzed using ImageJ 1.47v (Wayne Rasband, National Institute of Health, USA).

2.10 | Platelet activation measured by flow cytometry

As previously described,³⁴ washed human platelets were stimulated with 1 unit/mL of thrombin or 5 μg/mL of

cross-linked collagen-related peptide (CRP-XL) and fixed in 1% w/v paraformaldehyde for 30 minutes. After diluting 1 in 10 in modified Tyrode's buffer, fluorescein isothiocyanate (FITC)-conjugated anti-activated integrin αIIbβ3 (PAC-1, #340507, BD Biosciences) or phycoerythrin (PE)-conjugated anti-P-selectin (#561921, BD Biosciences) was used to stain platelets and fluorescence staining was assessed using a FACS Aria III flow cytometer (BD Biosciences).

2.11 | Pharmacological treatment of mice

Drug administration was obtained by mixing either 2APT or 2APT-D6 (in 2% v/v dimethyl sulfoxide (DMSO)) with solid food to reach a daily dose of 20, 60 or 200 mg of medication per kg of mouse body weight. About 2% v/v DMSO vehicle solution was used as a negative control. All in vivo studies are in accordance with ARRIVE guidelines and were performed according to local ethical approval (University of Exeter) and Home Office licensing for Scientific Procedures (PPL30/3348). All animal procedures conformed to the guidelines from Directive 2010/63/EU of the European Parliament on the protection of animals used for scientific purposes. Euthanasia was obtained by neck dislocation under 1.5%-2% isoflurane anesthesia.

2.12 | Liquid chromatography-mass spectrometry to detect 2APT and derivatives in vivo

Organ homogenates or plasma were precleared by acetonitrile 1:1 precipitation. The QTOF-UHPLC analysis was conducted using a MaXis HD quadrupole electrospray time-of-flight (ESI-QTOF) mass spectrometer (Bruker Daltonik GmbH, Bremen, Germany), operated in ESI positive-ion mode. The capillary voltage was set to 4500 V, nebulizing gas at 4 bar, drying gas at 12 L/min at a drying temperature of 220°C. Mobile phases A and B consisted of 0.1% v/v formic acid in water and 0.1% v/v formic acid in acetonitrile, respectively. Gradient elution was carried out with 10% mobile phase B for 2 minutes followed by a linear gradient to 99% B until 8 minutes, then returned to 10% B in 12 minutes total run time. The mass calibrant solution consisted of three parts of 1 M NaOH to 97 parts of 50:50 water:isopropanol with 0.2% formic acid. 2APT was detected as [M]⁺ and [M + H]⁺ ions at 241.0556 and 242.0634 m/z. Data processing was performed using the Data Analysis software version 4.3 (Bruker Daltonik GmbH, Bremen, Germany).

2.13 | Statistical analysis

For dual comparisons of normal/homoscedastic data, statistical analysis was performed by one-tailed unpaired t-tests.

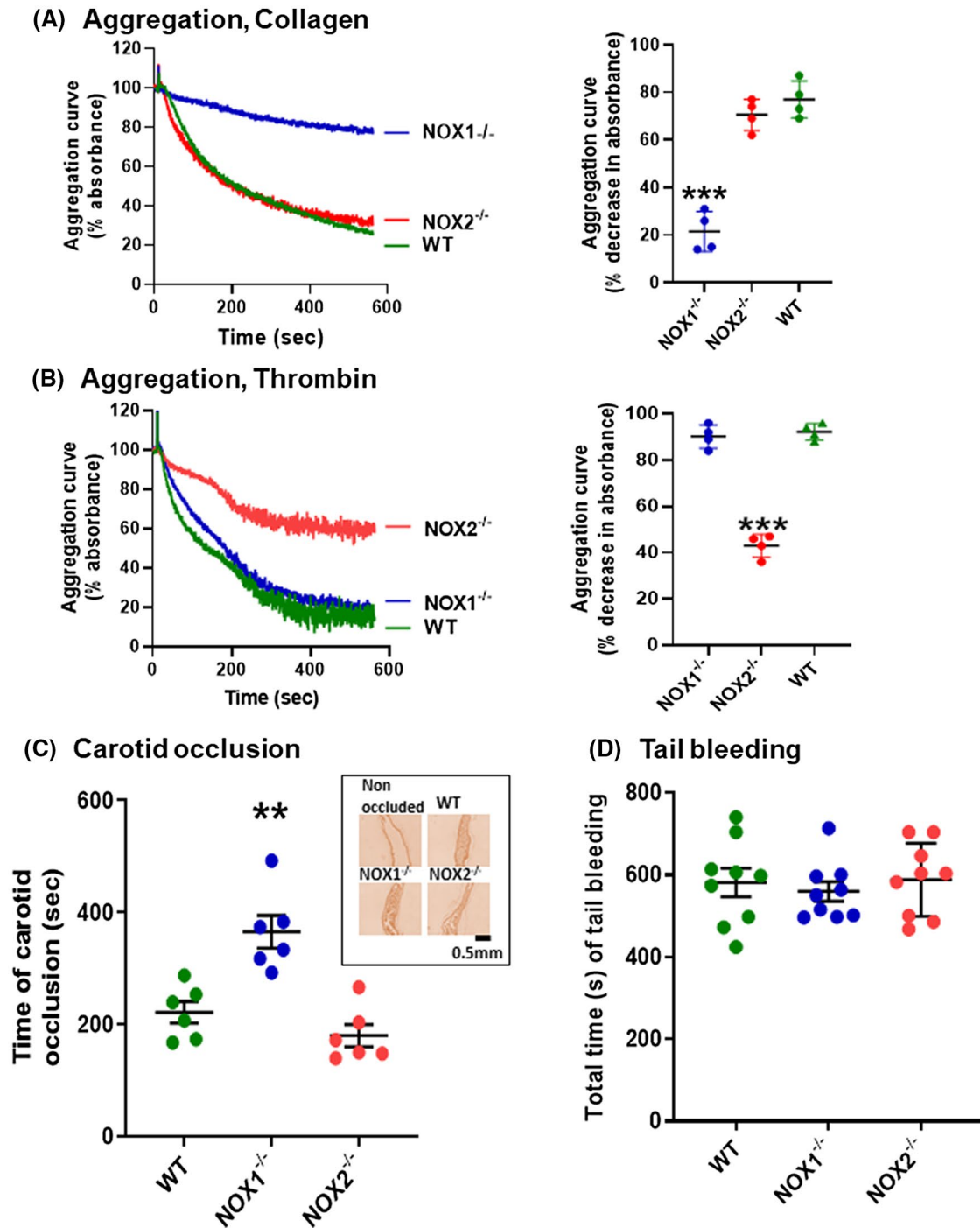


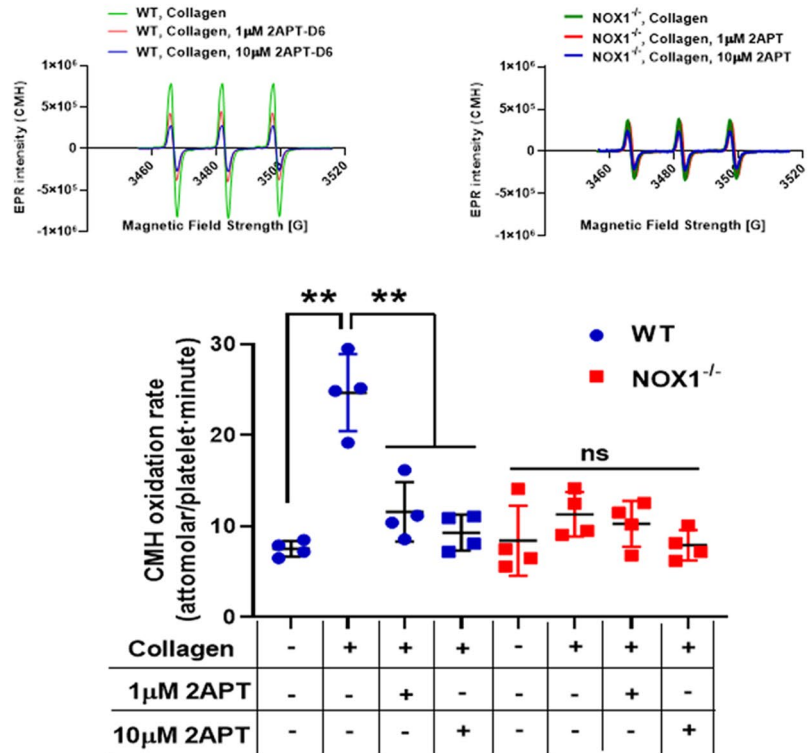
FIGURE 2 NOX1 positively regulates collagen-dependent activation of platelets and facilitates carotid occlusion in vivo. Platelets were isolated from NOX1^{-/-}, NOX2^{-/-}, and wild-type mice (WT, C57BL/6J) and resuspended at 2×10^8 cells/mL. Aggregation was obtained with $3 \mu\text{g}/\text{mL}$ of collagen (A) or 0.1 unit/mL of thrombin (B) and measured for up to 10 minutes. Traces shown on the left are representative of 4 independent experiments, while quantitative analysis is shown on the right. NOX1^{-/-}, NOX2^{-/-}, and WT mice were also tested in a ferric chloride-induced carotid occlusion assay. The time required for complete occlusion from 6 animals is displayed in (C), while hematoxylin staining of explanted carotid sections after ferric chloride treatment is shown in the insert. The hemostatic response was assessed with a tail tip transection assay and the time necessary for complete interruption of the bleeding from 9 animals per genotype is shown in (D). Statistical analysis was performed by one-way ANOVA with Bonferroni post-test (* for $P < .05$, ** for $P < .01$, *** for $P < .001$, ns for non-significant)

Dual comparisons of non-normal/non-homoscedastic data were analyzed by one-tailed non-parametric Mann-Whitney test. One-way analysis of variance (ANOVA) with Bonferroni

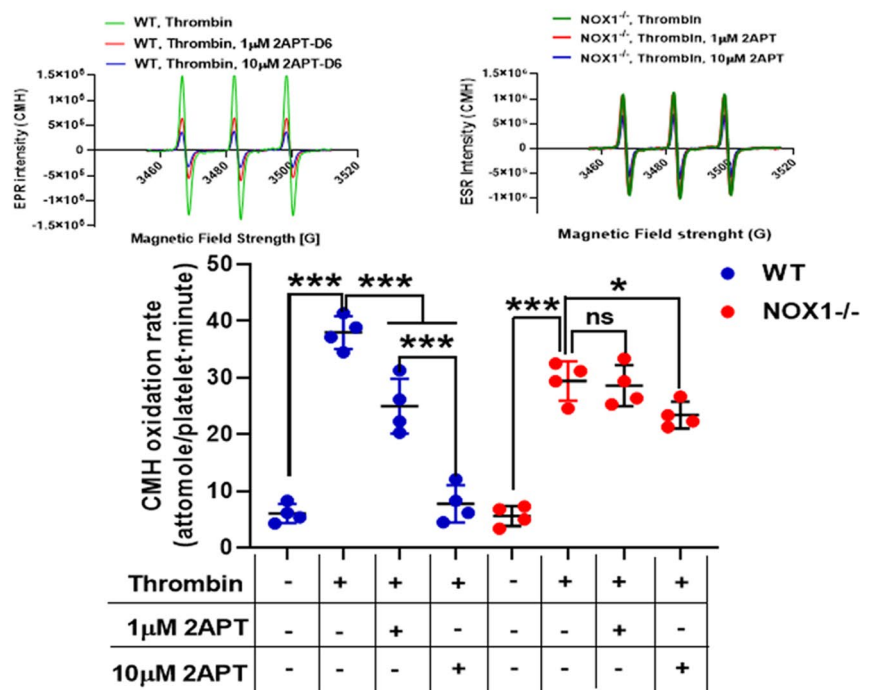
post-test was used for multiple comparison tests of normal/homoscedastic data. Data normality and homoscedasticity were tested with Shapiro-Wilk and Bartlett's tests, respectively.

FIGURE 3 2APT selectively inhibits NOX1 in superoxide anion formation assays. Platelets were isolated from NOX1^{-/-} and WT mice (C57BL6/J) and resuspended at 2 × 10⁸ cells/mL. Superoxide anion output was measured by EPR following platelet activation with 3 μg/mL of collagen (A) or 0.1 unit/mL of thrombin (B) and measured for 10 minutes. Platelets were pretreated with 0, 1 or 10 μM 2APT for 10 minutes. The amount of oxidized CMH was quantified as described in the Methods and in Figure S1 and expressed as attomoles of CMH oxidized per platelet per minute. Data from 4 independent experiments are shown, while representative EPR traces are shown in the upper panels. Statistical analysis was performed by one-way ANOVA with Bonferroni post-test (* for *P* < .05, ** for *P* < .01, *** for *P* < .001, ns for non-significant)

(A) EPR, Collagen

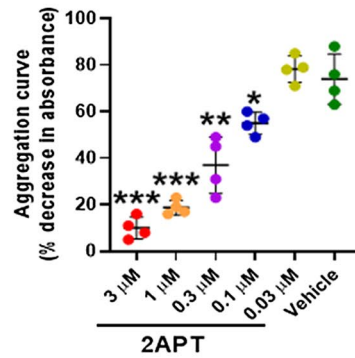
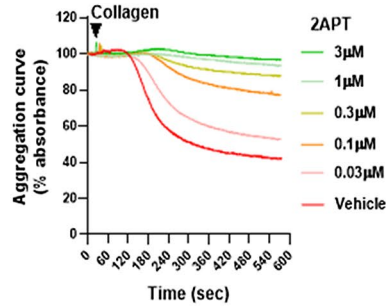
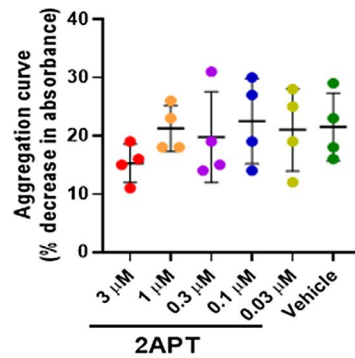
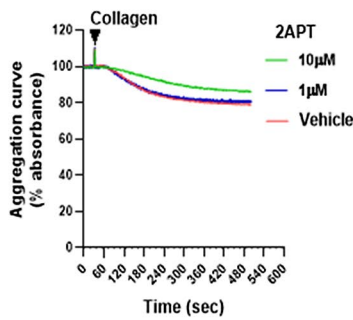
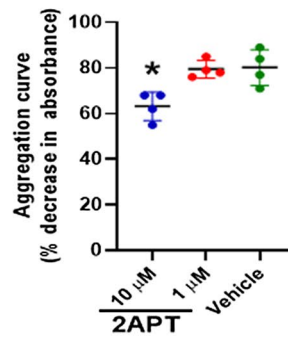
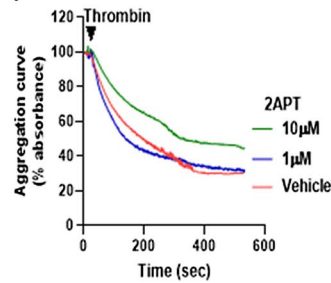
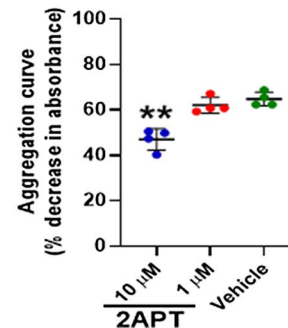
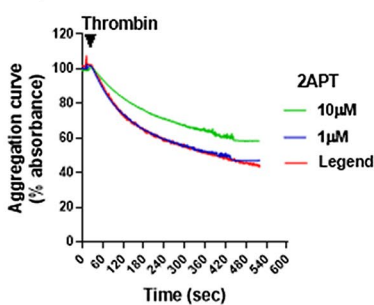


(B) EPR, Thrombin



Static adhesion experiments were normalized and analyzed by one-sample t-test vs 100% for the untreated condition. The statistical software package GraphPad Prism Version 8.1.0

for Windows 64 bit was used. Results were expressed as the mean ± standard error (SEM). Differences were considered significant at *P* value < .05 (*), .01 (**), or .001 (***).

(A) Aggregation, Collagen**i) WT****ii) NOX1^{-/-}****(B) Aggregation, Thrombin****i) WT****ii) NOX1^{-/-}****3 | RESULTS**

Thrombin- and collagen-induced aggregation experiments using platelets from NOX1^{-/-} and NOX2^{-/-} mice showed that collagen-induced aggregation is significantly inhibited in NOX1^{-/-} (Figure 2A), while thrombin-induced

FIGURE 4 2APT selectively inhibits platelet aggregation in a NOX1-dependent manner. Mouse platelet aggregation was stimulated with 3 μg/mL of collagen (A) or 0.1 unit/mL of thrombin (B). A concentration-inhibition curve for 2APT on collagen calculated with data shown here in Figure 3Ai can be found in Figure 6Ai. WT (i) and NOX1^{-/-} (ii) platelets were tested following treatment with 2APT for 10 minutes (0, 0.03, 0.1, 0.3, 0.3, 1 and 3 in Ai, and 0, 1 and 10 μM in Aii, Bi and Bii). Data from 4 independent experiments are shown on the right, while representative aggregation curves are shown on the left. Statistical analysis was performed by one-way ANOVA with Bonferroni post-test (* for $P < .05$, ** for $P < .01$, *** for $P < .001$, ns for non-significant)

aggregation is significantly reduced in NOX2^{-/-} platelets (Figure 2B). Carotid occlusion (Figure 2C, and representative traces in Figure S2) and tail tip transection bleeding time (Figure 2D) showed that NOX1^{-/-} mice have significantly delayed carotid occlusion compared to wild-type mice, while tail bleeding is not affected. The response of NOX2^{-/-} mice

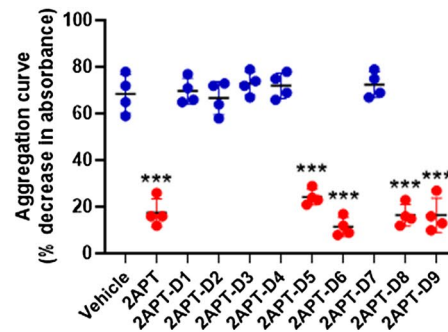
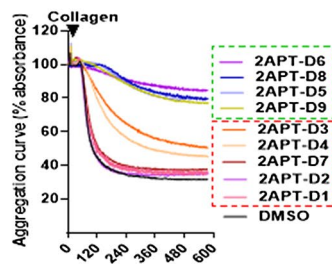
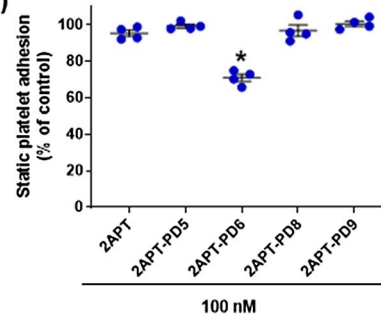
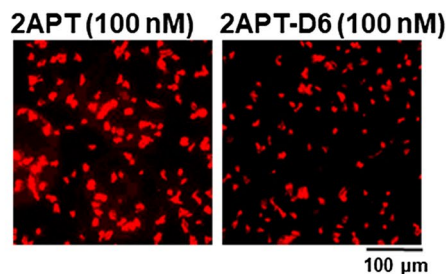
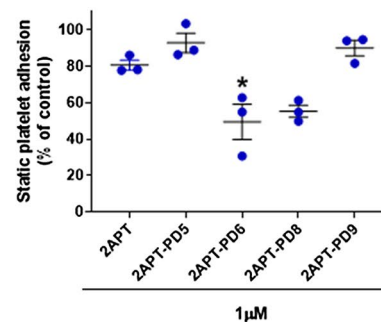
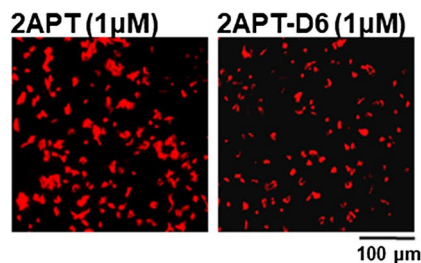
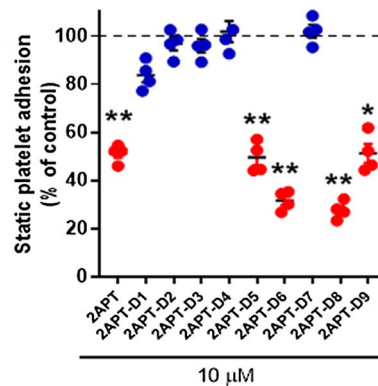
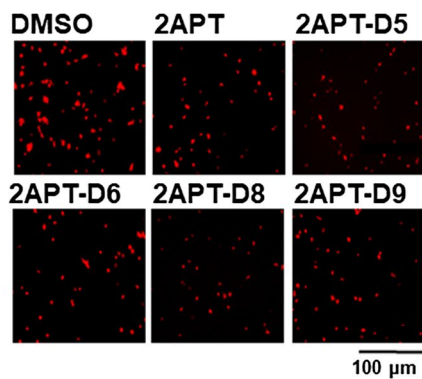
(A) Aggregation, Collagen**(B) Adhesion, Collagen**

FIGURE 5 2APT derivatives inhibit aggregation and static adhesion of human platelets in response to collagen. Human washed platelets were resuspended at 2×10^8 cells/mL for aggregation experiments or 2×10^7 cells/mL for adhesion experiments. Platelets were incubated 10 minutes with $10 \mu\text{M}$ 2APT, 2APT-D1, 2APT-D2, 2APT-D3, 2APT-D4, 2APT-D5, 2APT-D6, 2APT-D7, 2APT-D8 or 2APT-D9. Aggregation was induced by $3 \mu\text{g/mL}$ of collagen (A, representative left and quantification right, $n = 4$). Static adhesion on collagen-coated surfaces in the presence of 2APT and derivatives was tested by fluorescence microscopy and quantified for area coverage. After initial testing of all derivatives at concentration $10 \mu\text{M}$, only 2APT, 2APT-D5, 2APT-D6, 2APT-D8 or 2APT-D9 were studied at lower concentrations ($1 \mu\text{M}$ and 100 nM). Representative micrographs are shown on the left, while the quantification of the results is shown the right. Data were normalized to the control value in the absence of NOX1 inhibitors and expressed as % of surface area coverage in the absence of inhibitors. For the entire figure, $n = 4$ and statistical analysis were analyzed by one-way ANOVA with Bonferroni post-test (* for $P < .05$, ** for $P < .01$, *** for $P < .001$, ns for non-significant)

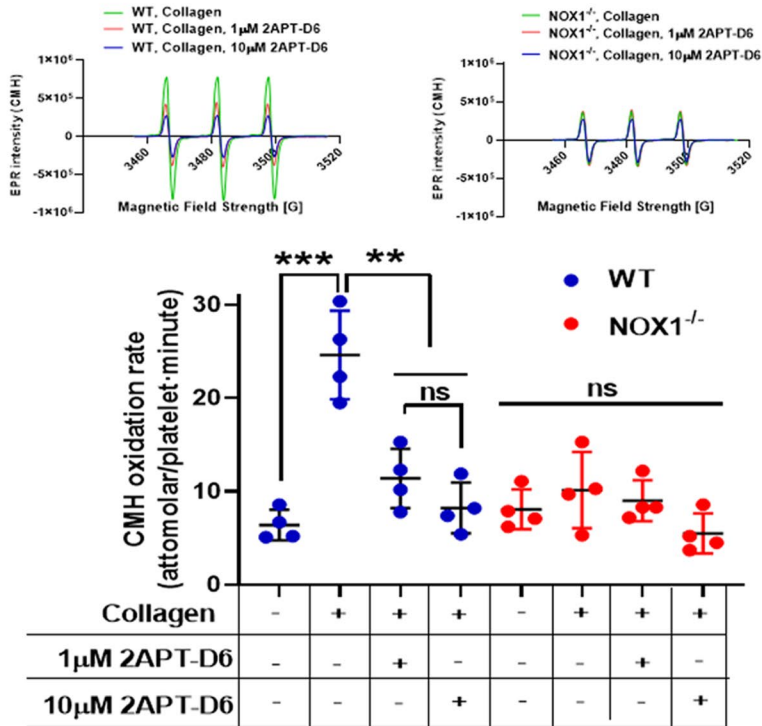
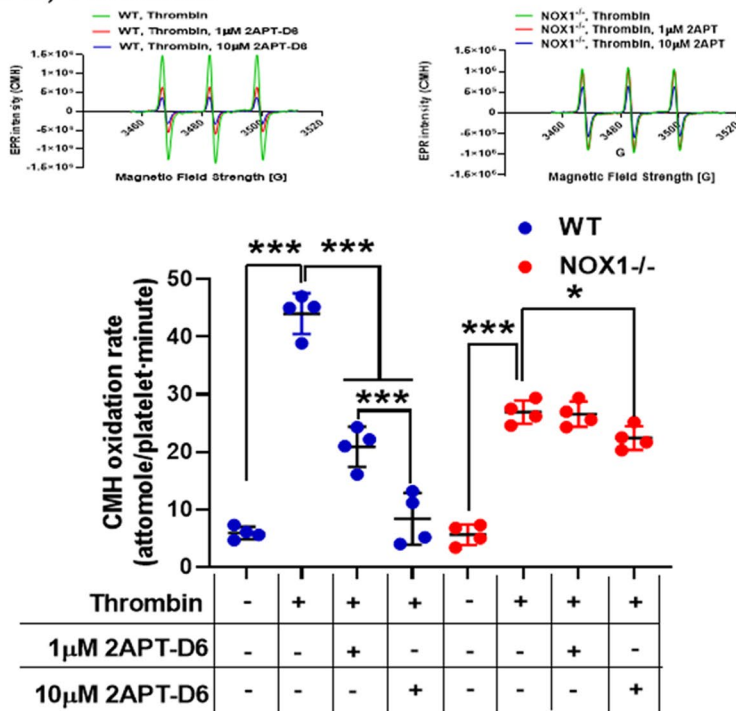
(A) EPR, Collagen

FIGURE 6 Characterization of 2APT-D6 by superoxide anion formation assays. For EPR experiments, mouse platelets were isolated from NOX1^{-/-} and WT mice (C57BL6/J) and resuspended at 2×10^8 cells/mL. Superoxide anion output was measured by EPR following platelet activation with 3 μg/mL of collagen (A) or 0.1 unit/mL of thrombin (B) and measured for 10 minutes. Platelets were pretreated with 0, 1 or 10 μM 2APT for 10 minutes. The amount of oxidized CMH was quantified as described in the Methods and in Figure S1 and expressed as attomoles of CMH oxidized per platelet per minute. Data analysis from 4 independent experiments is shown, while representative EPR traces are shown in top panels. Statistical analysis was performed by one-way ANOVA with Bonferroni post-test (* for $P < .05$, ** for $P < .01$, *** for $P < .001$, ns for non-significant)

(B) EPR, Thrombin

was similar to wild-type controls for both carotid occlusion and tail bleeding.

NOX1 selectivity of 2-acetylphenothiazine (2APT) was then confirmed using electron paramagnetic resonance (EPR) spectroscopy.¹⁴ The calibration curve utilized to quantify the superoxide anion output is shown in Figure S1. In these

experiments, 2APT significantly inhibited the superoxide anion generation induced by collagen on wild-type platelets, but not in NOX1^{-/-} platelets (Figure 3A). The superoxide anion generation in response to thrombin was also inhibited by 2APT, although 1 μM was only marginally effective compared to 10 μM (~25% inhibition vs ~80%, Figure 3B). The

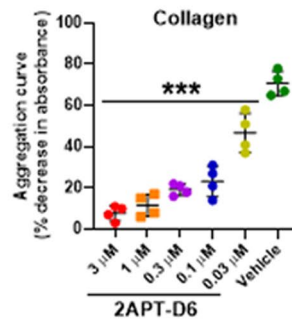
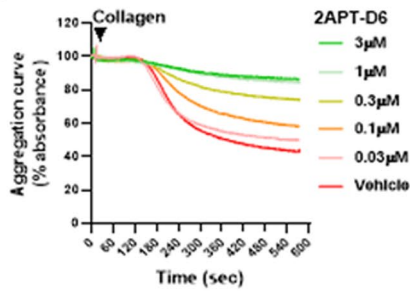
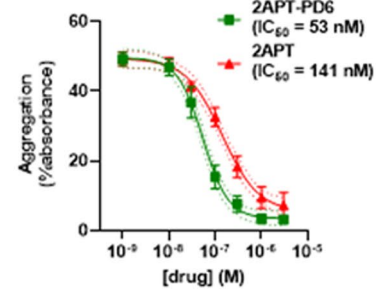
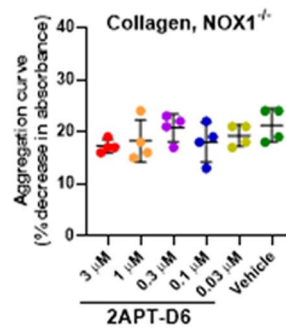
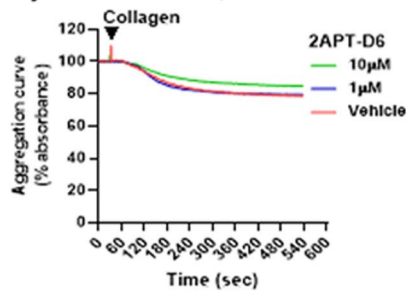
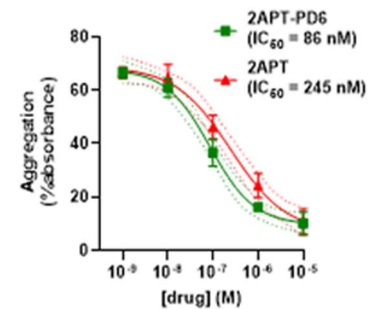
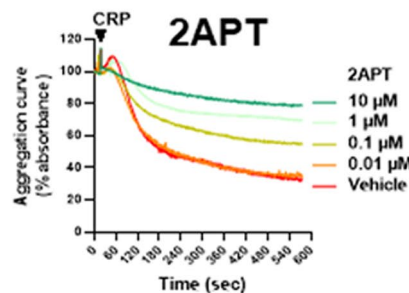
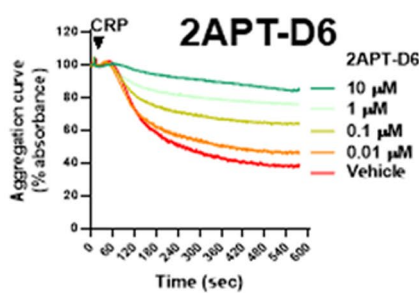
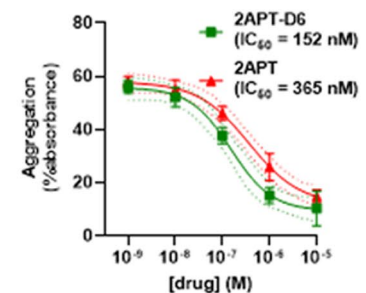
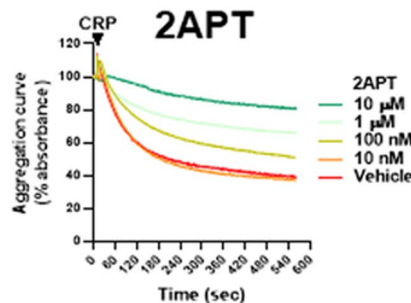
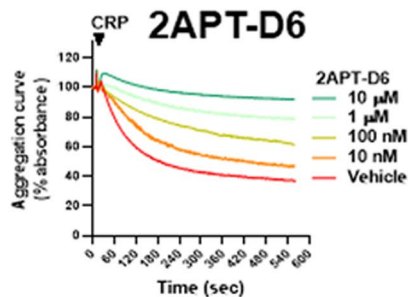
(A) Aggregation, Collagen**i) 2APT-D6, WT****ii) WT, 2APT vs 2APT-D6****iii) 2APT-D6, NOX1^{-/-}****(B) Aggregation, Mouse, CRP-XL****(C) Aggregation, Human, CRP-XL**

FIGURE 7 2APT and 2APT-D6 inhibit aggregation in a NOX1- and GPVI-manner in mouse and human platelets. Platelet aggregation was stimulated with 3 $\mu\text{g}/\text{mL}$ of collagen (A) or 1 $\mu\text{g}/\text{mL}$ of CRP-XL (B and C). WT (Ai) and NOX1^{-/-} (Aiii) mouse platelets were tested by turbidimetry following treatment with 2APT-6 for 10 minutes (0, 0.03, 0.1, 0.3, 0.3, 1, 3 or 10 μM). Concentration-inhibition curves for 2APT-D6 and 2APT (from data in Figure 3Ai) in WT mouse platelets are shown in Aii. In addition, 2APT-D6 and 2APT were tested for their effect on WT mouse (B) and human (C) platelet aggregation induced by 1 $\mu\text{g}/\text{mL}$ of CRP-XL. Representative examples from 3 independent experiments and their quantification are shown. The aggregation values at 9 minutes were fitted to a variable slope sigmoidal concentration-response to obtain IC₅₀ values for 2APT and 2APT-D6 (in red and green, respectively). Statistical analysis was performed by one-way ANOVA with Bonferroni post-test (* for $P < .05$, ** for $P < .01$, *** for $P < .001$, ns for non-significant)

inhibitory effect at 10 μM 2APT was detectable in $\text{NOX1}^{-/-}$ platelets stimulated by thrombin (Figure 3B).

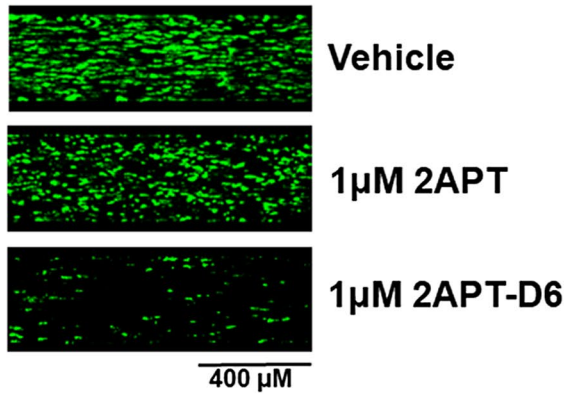
2APT was shown to inhibit collagen-dependent aggregation of wild-type platelets in a concentration-dependent manner (Figure 4Ai), while the effect in $\text{NOX1}^{-/-}$ was apparent only at 10 μM (Figure 4Aii). Moreover, thrombin-dependent

aggregation in wild-type and $\text{NOX1}^{-/-}$ platelets was only marginally affected by 2APT and only at the highest concentration (10 μM) (Figure 4Bi,ii).

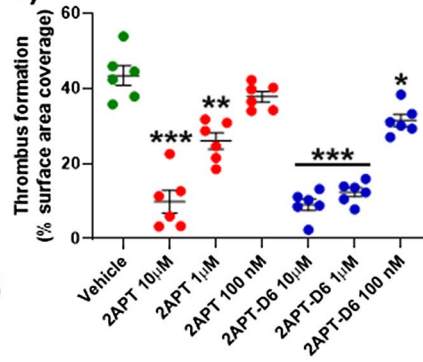
In order to improve 2APT selectivity (by increasing the potency of NOX1 inhibition) and bioavailability (by increasing the hydrophilicity of the drug), a group of synthetic

(A) Thrombus formation, Collagen

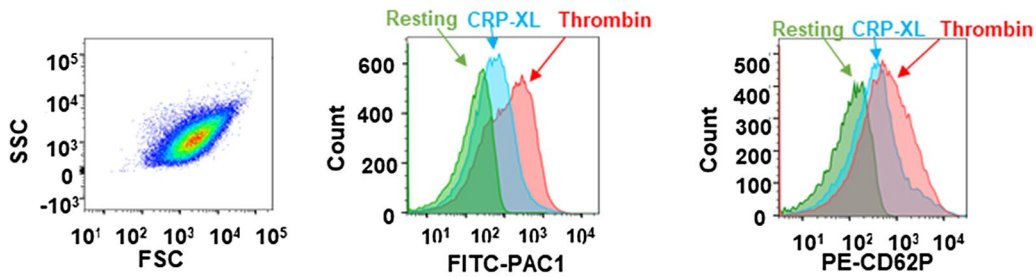
i)



ii)

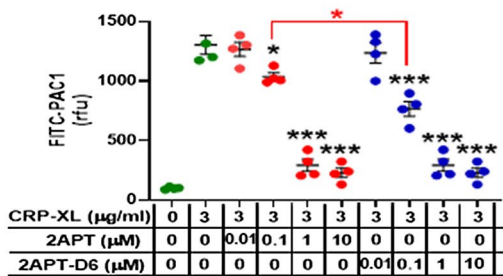


(B) Flow cytometry

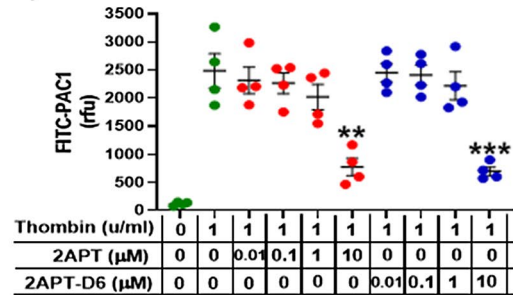


(C) Flow cytometry, integrin $\alpha\text{IIb}\beta\text{3}$ activation

i) CRP-XL

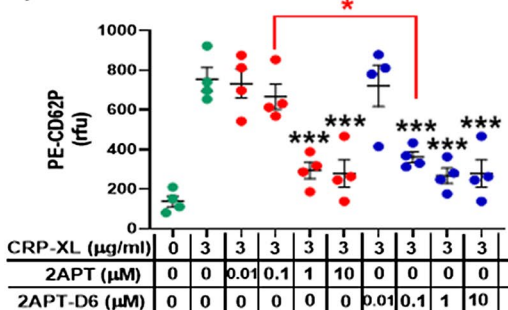


ii) Thrombin



(D) Flow cytometry, P-selectin externalization

i) CRP-XL



ii) Thrombin

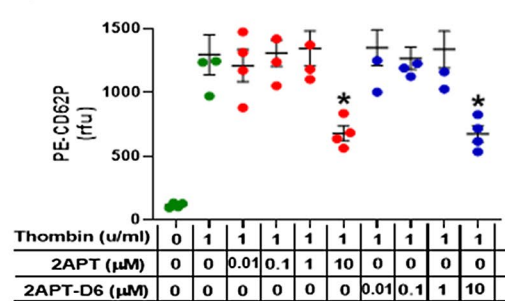


FIGURE 8 2APT and 2APT-D6 inhibit collagen-dependent thrombus formation, integrin α Ib β 3 activation, and P-selectin externalization. 2APT and 2APT-D6 were compared in whole blood thrombus formation assays under shear stress (A). The compounds were incubated for 10 minutes at concentrations 0.1, 1 and 10 μ M on whole blood from human healthy volunteers where platelets were stained by DiOC6. The flow was applied for 10 minutes (1000 sec^{-1}) before fluorescence pictures of the surfaces were taken to reveal the formation of thrombi. Representative examples for drug concentration 1 μ M are shown in Ai, while statistical analysis for all drug concentrations is shown Aii ($n = 6$, one-way ANOVA with Bonferroni post-test, * for $P < .05$, ** for $P < .01$, *** for $P < .001$, ns for non-significant). For flow cytometry, platelets were isolated from human blood, resuspended at 2×10^7 cells/mL, and activated with 3 μ g/mL of CRP-XL or 1 unit/mL of thrombin in static conditions. The platelet population analyzed by flow cytometry is shown in B (forward scattering vs side scattering plot, left panel). Integrin α Ib β 3 activation (B, central panel) and P-selectin externalization (B, right panel) were analyzed by staining with activated α Ib β 3 (PAC-1) and P-selectin antibodies followed by flow cytometry. Platelets were incubated 10 minutes with 0, 0.01, 0.1, 1 or 10 μ M of 2APT or 2APT-D6 before stimulation and immunostaining. The effect of 2APT and 2APT-D6 on integrin α Ib β 3 activation (C) and P-selectin externalization (D) in response to CRP-XL (i) and thrombin (ii) is shown (mean \pm SEM, $n = 4$). Statistical analysis was performed by one-way ANOVA with Bonferroni post-test, * for $P < .05$, ** for $P < .01$, *** for $P < .001$, ns for non-significant. Although results for 2APT and 2APT-D6 are similar, the effect of the compounds at concentration 0.1 μ M is statistically different (2APT-D6 causes more extensive inhibition, red lines, and asterisk to indicate $P < .05$)

derivatives was synthesized and examined in this study (2APT-D1/9). The nine derivatives are in Figure 1 (including their calculated hydrophobicity cLogP) and their syntheses are described in the Supplementary Methods. All nine newly synthesized compounds were tested in platelet aggregation experiments, where only 2APT, 2APT-D5, 2APT-D6, 2APT-D8, and 2APT-D9 inhibited responses induced by 3 μ M collagen, while 0.1 unit/mL of thrombin was not affected (Figure 5A and Figure S3A, respectively). Similarly, a static platelet adhesion assay on collagen confirmed the activity of 2APT-D5, 2APT-D6, 2APT-D8, and 2APT-D9 (Figure 5B). The active derivatives 2APT-D5, 2APT-D6, 2APT-D8, and 2APT-D9 were further tested by static adhesion onto collagen at a concentration of 1 μ M and 100 nM, at which only 2APT-D6 significantly inhibited platelet adhesion (Figure 5B). In parallel, neither 2APT nor its derivatives inhibit platelet adhesion to fibrinogen (Figure S3B).

Using EPR, we found that: (1) 2APT-D6 at a concentration of 1 or 10 μ M reduces superoxide anion formation in response to collagen extensively (Figure 6A); (2) NOX1 specificity cannot be tested in NOX1^{-/-} platelet stimulated by collagen as the agonist-induced superoxide generation is absent (Figure 6A); (3) the inhibition of superoxide generation in response to thrombin is significantly higher for 10 μ M than 1 μ M 2APT-D6 in wild-type mouse platelets (~85% inhibition vs ~50%, Figure 6B); (4) only 10 μ M but not 1 μ M 2APT-D6 has a minor inhibitory effect on thrombin-dependent superoxide generation in NOX1^{-/-} (Figure 6B).

In aggregation assays, 2APT-D6 inhibited collagen-induced WT mouse platelet aggregation in a concentration-dependent manner (Figure 7Ai), with higher potency than 2APT (IC₅₀ = 52 \pm 18 nM vs 141 \pm 42 nM, Figure 7Aii). NOX1^{-/-} platelets were tested resulted insensitive to 2APT-D6 except for the highest concentration of 10 μ M (Figure 7Aiii). Both 2APT-D6 and 2APT inhibited mouse platelet aggregation induced by the GPVI-selective agonist CRP-XL,³⁵ with IC₅₀ of 77 \pm 24 nM and 179 \pm 37 nM, respectively (Figure 7B). CRP-XL aggregation experiments were repeated

on human platelets, confirming higher potency for 2APT-D6 over 2APT (145 \pm 25 vs 383 \pm 5 nM, Figure 7C).

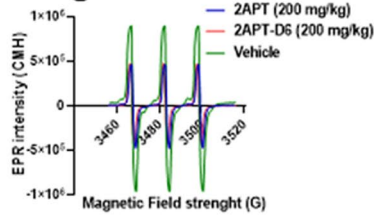
Either 2APT-D6 or 2APT inhibited collagen-dependent thrombus formation underflow, although a significantly higher inhibition was detected for 2APT-D6 at 100 nM compared to 2APT (Figure 8A). Integrin α Ib β 3 activation and P-selectin externalization (ie, degranulation) in response to 3 μ g/mL of CRP-XL were also inhibited by both 2APT-D6 (blue symbols) and 2APT (red symbols) (Figure 8Ci,Di, respectively). Notably, 2APT-D6 appeared significantly more effective at 0.1 μ M than 2APT (red connector lines and asterisks). Both activation of α Ib β 3 and P-selectin externalization in response to 1 unit/mL of thrombin were inhibited only by the highest tested concentration for both compounds (ie, 10 μ M, Figure 8Cii,Dii, respectively).

The compounds were then administered in mice via the diet by mixing ground chow diet pellet with drug solution (in 2% v/v dimethyl sulfoxide) in order to obtain a daily dose of 20, 60 or 200 mg/kg. After two full days of treatment, washed platelets were tested by EPR, which showed significant inhibition of collagen-dependent superoxide generation, while the thrombin-dependent superoxide output was not affected (Figure 9A). In parallel, washed platelet turbidimetry showed that both compounds comprehensively inhibit collagen-dependent aggregation (Figure 9Bi), but have no effect on thrombin-dependent aggregation (Figure 9Bii).

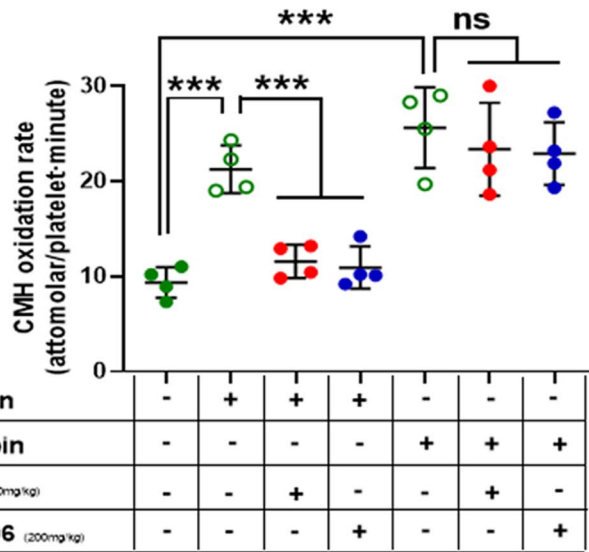
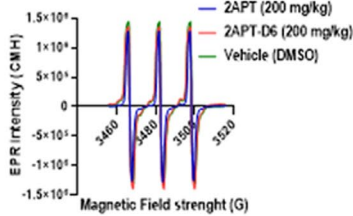
Whole blood from mice that received the compounds orally was tested for thrombus formation on collagen in the absence of coagulation and under physiological flow (1000 sec^{-1}). Either 2APT or 2APT-D6 at 200 mg/kg daily dose comprehensively abolished thrombus formation. When tested at different daily doses (60 and 20 mg/kg), 2APT and 2APT-D6 showed a similar dose-dependence, with 25%-30% inhibition of thrombus formation by 60 mg/kg and no effect by 20 mg/kg (Figure 10A). The induction of carotid occlusion by ferric chloride was also significantly delayed by 200 mg/kg daily doses of 2APT- and 2APT-D6 (Figure 10B), while no significant effects were

(A) EPR

Collagen

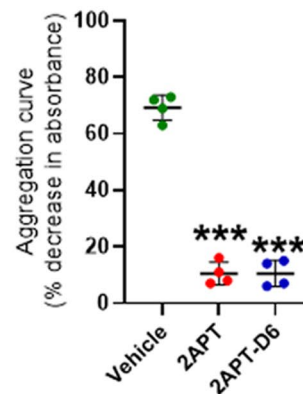
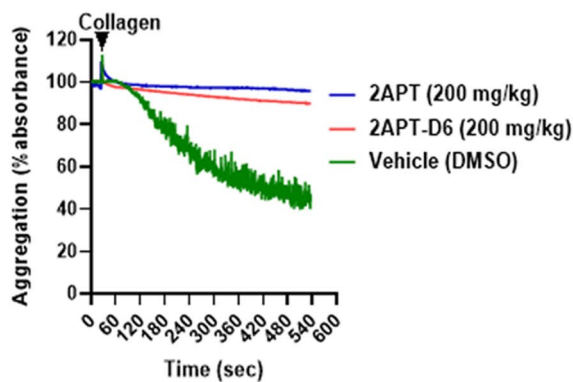


Thrombin



(B) Aggregation

i) Collagen



ii) Thrombin

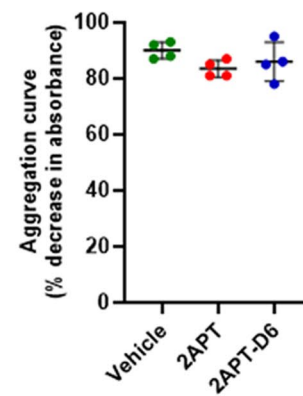
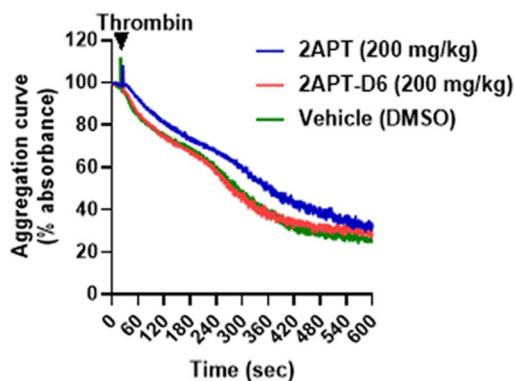


FIGURE 9 In vivo administration of 2APT and 2APT-D6 selectively inhibits collagen-dependent superoxide anion formation and platelet aggregation. The drugs were administered in food (daily dose = 200 mg/kg). Control animals only received vehicle solution mixed with their food (2% v/v DMSO). Superoxide anion formation in response to 3 μ g/mL of collagen or 0.1 unit/mL of thrombin was measured for 10 minutes by EPR spectrometry (statistical analysis and representative examples are shown in A). Collagen- and thrombin-dependent aggregation were measured by turbidimetry (Bi and Bii, respectively). Representative example of aggregation curves are shown on the left and statistical analysis is shown on the right. Throughout this figure, statistical analysis was performed by one-way ANOVA with Bonferroni post-test ($n = 4$, * for $P < .05$, ** for $P < .01$, *** for $P < .001$, ns for non-significant)

detected for the daily dose of 20 mg/kg (data not shown). Notably, tail bleeding time assays were not affected by treatment with either 2APT or 2APT-D6 even at the highest daily dose of 200 mg/kg (Figure 10C). Finally, using liquid chromatography-mass spectrometry (LC-MS), 2APT was detected in plasma, kidney, and liver homogenates of C57BL6/J mice receiving the drug orally (Figure 10Di). C57BL6/J mice fed either 2APT or 2APT-D6 (200 mg/kg daily) showed detectable levels of 2APT but not 2APT-D6 (Figure 10Dii). A novel 2APT-glucose adduct was detected in the platelet-rich plasma of C57BL6/J mice fed either 2APT or 2APT-D6 (Figure 10Diii).

4 | DISCUSSION

Using NOX1^{-/-} and NOX2^{-/-} transgenic mice^{29,30} and a model of carotid occlusion induced by ferric chloride,³¹ we proved that NOX1 accelerates thrombosis. In parallel, hemostasis tested in tail tip transection assays³⁶ is unaffected by NOX1 deficiency. NOX1 is, therefore, a promising target for the development of pharmacological agents able to protect against thrombosis without increasing bleeding risk. Using washed platelets from NOX1^{-/-} and NOX2^{-/-} transgenic mice, we have also proved that NOX1 is critical for collagen responses, while the latter is required for thrombin responses. This is in agreement with previous studies,^{10,13,14} but in contrast with other reports.^{9,37} This discrepancy is difficult to explain, although it can be at least partially explained with the differences in experimental tools and conditions utilized. For example, the inhibitor peptide used as NOX2-specific by Cammisotto and colleagues³⁷ directly binds and competitively inhibits p47phox.³⁸ Therefore, in addition to inhibiting NOX2, this peptide can potentially inhibit the p47phox-dependent activation of other NOXs (including NOX1³⁹⁻⁴¹) and the results from this manuscript may be reinterpreted under a different light. Interestingly, our conclusions on the role of NOX1 in collagen signaling are in agreement with a recent paper showing no changes in platelet responses to collagen in NOX2^{-/-} mice and *Cybb* (NOX2)-mutation bearing granulomatous disease (CGD) patients.¹²

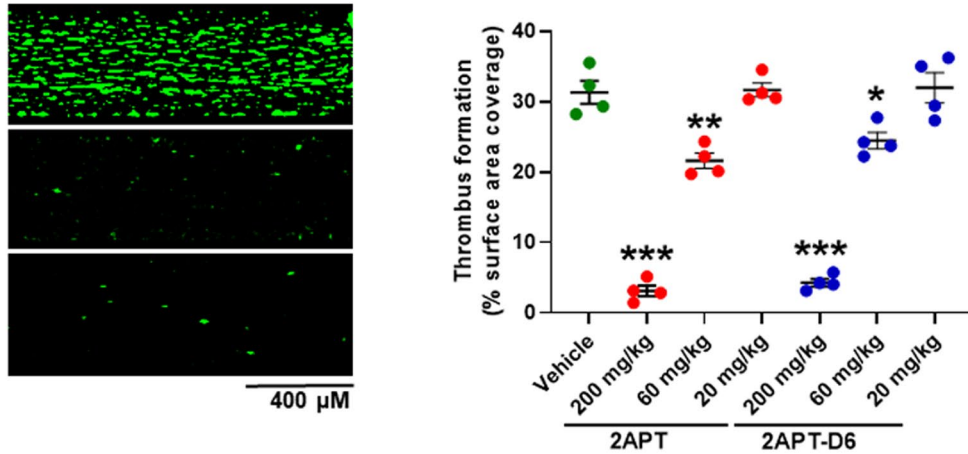
Our current data obtained with the GPVI-specific agonists CRP-XL are in agreement with previous literature suggesting a role for NOX1 in the regulation of the collagen receptor GPVI.^{10,13,14} Pharmacological inhibition of GPVI has been shown to reduce thrombotic responses without affecting hemostasis in a manner similar to what we observed for NOX1^{-/-} and GPVI targeting has previously been proposed as a potential strategy for the prevention of atherothrombosis.⁴² Because only peptides or antibodies with notable limitations about pharmacokinetics and deliverability have so far been successfully utilized as GPVI inhibitors,⁴³⁻⁴⁵ this receptor remains an interesting drug discovery target. In this

study, we investigated the possibility of targeting NOX1 and indirectly dampening GPVI signaling with small molecule inhibitors. A number of small molecule NOX inhibitors with isotype selectivity have recently been developed.^{19,21,46,47} We previously described the effect of the NOX1-selective inhibitor 2APT on platelets *ex vivo*.¹⁰ Here we further characterized the antiplatelet potential of 2APT both *ex vivo* and *in vivo*. In addition, in order to improve its water solubility and potency as NOX1 inhibitor (which would allow its use without the risk of reaching the threshold at which other NOXs are also affected), we designed, synthesized, and examined nine related chemical derivatives of 2APT. The 2APT derivatives 2, 3, and 7 possess modifications to the 2APT structure; however, the remaining derivatives all have the potential to release unmodified 2APT, via two different pathways. Specifically, derivatives 2APT-D1, 4, 5, 8, and 9 can undergo hydrolysis to afford a common β -keto acid intermediate that can then undergo enzymatic decarboxylation to release 2APT.⁴⁸ In an alternative approach, 2APT-D6 contains a vinyl *tert*-butyl carbonate that upon hydrolysis is able to afford 2APT *directly*. A similar prodrug approach using a *tert*-butyl carbonate motif was examined with orally administered entacapone and was reported to be quantitatively hydrolyzed to the drug in serum.⁴⁹ Interestingly, the potency of the derivatives studied here seems unrelated to their hydrophilicity and water solubility, with the most potent derivative 2APT-D6 *in vitro* markedly less hydrophilic than 2APT (ie, cLogP 4.39 vs 3.93). It was promising to see that 2APT and 2APT-D6 orally administered to mice significantly reduced platelet responses (ie, aggregation, superoxide anion formation, and thrombus formation underflow—Figure 7). This suggests that the compounds that are not degraded in the GI tract, are absorbed and reach the blood at concentrations compatible with their biological activity. 2APT could, in fact, be detected by mass spectrometry in kidney, liver, and platelet-rich plasma lysates of treated animals but not control animals that received vehicle solution (Figure 10D). The prodrug mechanism was confirmed by mass spectrometry experiments showing the parent molecule 2APT in animals treated with 2APT-D6. More surprising was the absence of 2APT-D6 from the plasma of mice receiving this compound as treatment. This may suggest that only 2APT is retained in the bloodstream and is the active compound for both 2APT and 2APT-D6 treatments. It was, therefore, not surprising to see no potency difference between these two inhibitors in our *in vivo* experiments. At this point, we can hypothesize that because of its hydrophobicity, 2APT-D6 either does not reach the bloodstream or is readily cleared from it. In addition, a novel molecule appeared in the plasma of animals treated with 2APT and 2APT-D6, which was identified as a 2APT-glucose adduct. Further studies on the relevance of this molecule for absorption and biological activity of 2APT and 2APT-D6 are required.

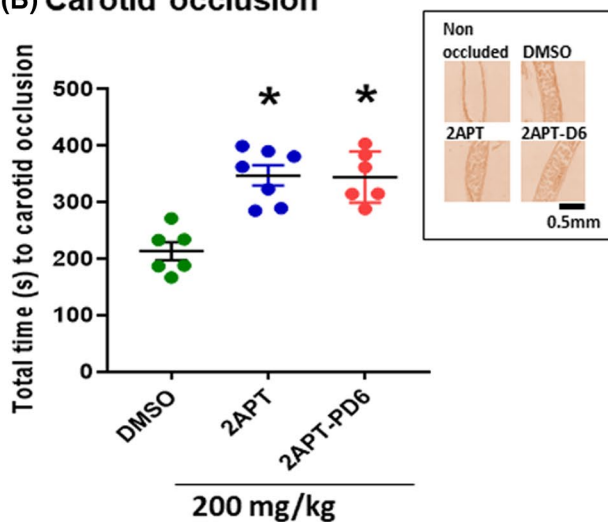
In summary, 2APT and 2APT-D6 selectively impair collagen-dependent activation of platelets via inhibition of NOX1 without affecting thrombin responses, which reduces thrombosis without attenuating hemostasis (Figure 11 for a schematic diagram). These compounds could, therefore, be developed into antiplatelet drugs without the unwanted side

effect of increasing bleeding risks,^{50,51} which is an unresolved weakness of existing drugs. The collagen receptor GPVI has been suggested as a potential antiplatelet drug target, but only two inhibitors reached an advanced development stage (ie, Revacept and ACT017).⁵² Therefore, the development of a small molecule drug targets GPVI and

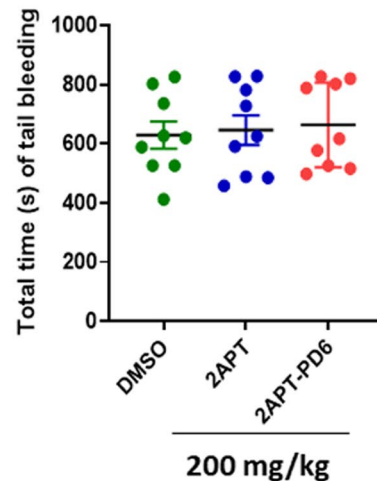
(A) Thrombus formation, Collagen



(B) Carotid occlusion



(C) Tail bleeding



(D) Mass spectrometry detection

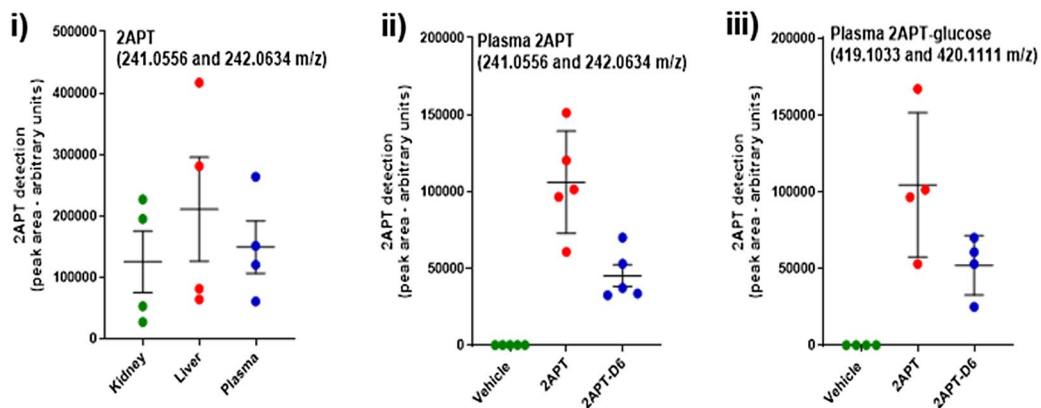


FIGURE 10 Administration of 2APT and 2APT-D6 reduces thrombus formation underflow and ferric chloride-induced carotid occlusion *in vivo*, but does not affect bleeding time in a tail tip transection assay. Drugs were administered in food (daily doses: 20, 60, and 200 mg/kg). Control animals only received vehicle solution mixed with their food (2% v/v DMSO). Whole blood thrombus formation under shear stress (1000 sec^{-1} for 10 minutes) was measured by DiOC6 platelet staining and fluorescence imaging. Representative results for 200 mg/kg and quantification of the surface area coverage for all three doses are shown (A, $n = 4$). Carotid occlusion was tested *in vivo* using a ferric chloride injury model (B). The time required for complete occlusion was plotted for vehicle-, 2APT- and 2APT-D6-treated animals ($n = 6$, mean \pm SEM). Confirmation of carotid occlusion was obtained by hematoxylin staining, of which representative examples are shown in the panel. The same treatments were assessed in a tail tip transection assays (C), in which the time required for full interruption of bleeding was recorded ($n = 9$, mean \pm SEM). 2APT detection by LC-MS in organs and plasma of animals treated orally (D). 2APT detection in organ homogenates of C57BL6/J mice fed 2APT is shown in (Di, $n = 4$). 2APT detection in platelet-rich plasma of C57BL6/J mice fed 2APT, 2APT-D6 or vehicle solution (2% v/v DMSO) is shown in (Dii, $n = 5$). A novel 2APT-glucose adduct was also detected in the platelet-rich plasma of C57BL6/J mice fed 2APT or 2APT-D6 but not vehicle solution (2% v/v DMSO) (Diii, $n = 4$). 2APT was detected as $[M]^+$ and $[M + H]^+$ ions at 241.0556 and 242.0634 m/z , while 2APT-glucose was detected as $[M]^+$ and $[M + H]^+$ ions at 419.1033 and 420.1111 m/z . Statistical analysis was performed by one-way ANOVA with Bonferroni post-test (* for $P < .05$, ** for $P < .01$, *** for $P < .001$, ns for non-significant)

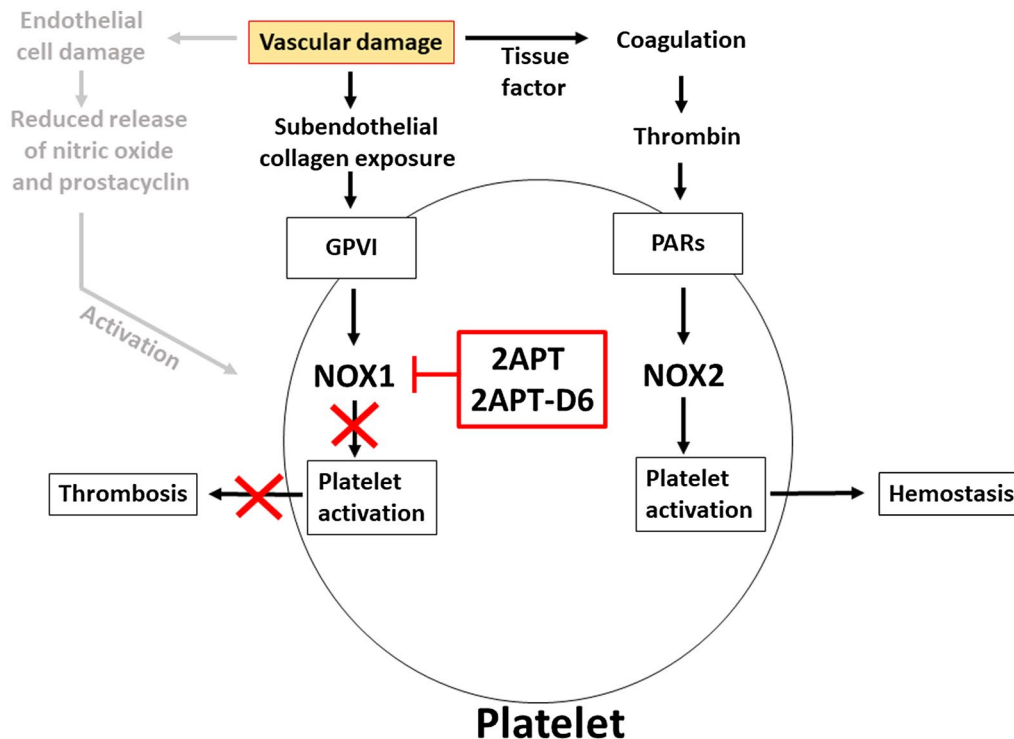


FIGURE 11 Graphical interpretation of the data presented in this manuscript. 2APT and 2APT-D6 selectively inhibit NOX1 and collagen-dependent platelet activation, while sparing thrombin responses. *In vivo*, this translates in the attenuation of thrombotic responses such as carotid occlusion depending on collagen-dependent platelet activation, while thrombin-dependent platelet activation guarantees sufficiently effective hemostasis as shown by unaffected tail bleeding time. 2APT = 2-acetylphenothiazine; 2APT-D6 = 2-acetylphenothiazine derivative 6; GPVI = glycoprotein VI; NOX = NADPH oxidase; PAR = protease-activated receptor

can be administered orally will be a great advance in the antithrombotic field.

ACKNOWLEDGMENTS

This work was funded by a British Heart Foundation grant (PG/15/40/31522) and Alzheimer Research UK (ARUK-PG2017A-3) to Giordano Pula. Work in Maarten Koeners' laboratory was supported by the British Heart Foundation (FS/14/2/30630 and PG/15/68/31717). The authors would also like to thank the Biological Service Unit of the University of Exeter for the *in vivo* work, the Clinical Research Facility

(CRF) of the University of Exeter and in particular Dr Bridget Knight for blood collections, the Chemical Characterization and Analysis Facility (CCAF) of the University of Bath (especially Dr Anneke Lubben and Dr Shaun Reeksting) for the mass spectrometry analysis, and Dr Bruno Fink from Noxygen Science Transfer & Diagnostics GmbH for the technical support. Open access funding enabled and organized by Projekt DEAL.

CONFLICT OF INTEREST

The authors declare no conflict of interest.

AUTHOR CONTRIBUTIONS

Dina Vara performed and analyzed the majority of the experiments, with help for in vivo treatment (Anuradha Tarafdar), platelet adhesion (Meral Celikag), and carotid occlusion assays (Daniela Patinha, Barbara Ferreira, and Zach Warren). Maarten P. Koeners supported the carotid occlusion experiments and participated in the preparation of the manuscript. Christina E. Gulacsy and Ellie Hounslea performed the synthesis of the novel compounds tested. Lorenzo Caggiano designed and synthesized the compounds, and participated in the writing of the manuscript. Giordano Pula designed the study, generated part of the data, analyzed all of the data, and wrote the manuscript.

DATA AVAILABILITY STATEMENT

Data in this article will be shared on request to the corresponding author by email.

REFERENCES

- El Haouari M. Platelet oxidative stress and its relationship with cardiovascular diseases in type 2 diabetes mellitus patients. *Curr Med Chem*. 2019;26:4145-4165.
- Ghasemzadeh M, Hosseini E, Roudsari ZO, Zadkhak P. Intraplatelet reactive oxygen species (ROS) correlate with the shedding of adhesive receptors, microvesiculation and platelet adhesion to collagen during storage: does endogenous ROS generation downregulate platelet adhesive function? *Thromb Res*. 2018;163:153-161.
- Monteiro PF, Morganti RP, Delbin MA, et al. Platelet hyperaggregability in high-fat fed rats: a role for intraplatelet reactive-oxygen species production. *Cardiovasc Diabetol*. 2012;11:5.
- Krotz F, Sohn HY, Gloe T, et al. NAD(P)H oxidase-dependent platelet superoxide anion release increases platelet recruitment. *Blood*. 2002;100:917-924.
- Magwenzi S, Woodward C, Wraith KS, et al. Oxidized LDL activates blood platelets through CD36/NOX2-mediated inhibition of the cGMP/protein kinase G signaling cascade. *Blood*. 2015;125:2693-2703.
- Gray SP, Di Marco E, Okabe J, et al. NADPH oxidase 1 plays a key role in diabetes mellitus-accelerated atherosclerosis. *Circulation*. 2013;127:1888-1902.
- Begonja AJ, Gambaryan S, Geiger J, et al. Platelet NAD(P)H-oxidase-generated ROS production regulates alphaIIb beta3-integrin activation independent of the NO/cGMP pathway. *Blood*. 2005;106:2757-2760.
- Vara D, Cifuentes-Pagano E, Pagano PJ, Pula G. A novel combinatorial technique for simultaneous quantification of oxygen radicals and aggregation reveals unexpected redox patterns in the activation of platelets by different physiopathological stimuli. *Haematologica*. 2019;104:1879-1891.
- Delaney MK, Kim K, Estevez B, et al. Differential roles of the NADPH-oxidase 1 and 2 in platelet activation and thrombosis. *Arterioscler Thromb Vasc Biol*. 2016;36:846-854.
- Vara D, Campanella M, Pula G. The novel NOX inhibitor 2-acetylphenothiazine impairs collagen-dependent thrombus formation in a GPVI-dependent manner. *Br J Pharmacol*. 2013;168:212-224.
- Violi F, Pignatelli P. Platelet NOX, a novel target for anti-thrombotic treatment. *Thromb Haemost*. 2014;111:817-823.
- Sonkar VK, Kumar R, Jensen M, et al. Nox2 NADPH oxidase is dispensable for platelet activation or arterial thrombosis in mice. *Blood Adv*. 2019;3:1272-1284.
- Walsh TG, Berndt MC, Carrim N, Cowman J, Kenny D, Metharom P. The role of Nox1 and Nox2 in GPVI-dependent platelet activation and thrombus formation. *Redox Biol*. 2014;2:178-186.
- Abubaker AA, Vara D, Eggleston I, Canobbio I, Pula G. A novel flow cytometry assay using dihydroethidium as redox-sensitive probe reveals NADPH oxidase-dependent generation of superoxide anion in human platelets exposed to amyloid peptide beta. *Platelets*. 2019;30:181-189.
- Carnevale R, Loffredo L, Sanguigni V, et al. Different degrees of NADPH oxidase 2 regulation and in vivo platelet activation: lesson from chronic granulomatous disease. *J Am Heart Assoc*. 2014;3:e000920.
- Kwon G, Uddin MJ, Lee G, et al. A novel pan-Nox inhibitor, APX-115, protects kidney injury in streptozotocin-induced diabetic mice: possible role of peroxisomal and mitochondrial biogenesis. *Oncotarget*. 2017;8:74217-74232.
- Wingler K, Altenhoefer SA, Kleikers PW, Radermacher KA, Kleinschnitz C, Schmidt HH. VAS2870 is a pan-NADPH oxidase inhibitor. *Cell Mol Life Sci*. 2012;69:3159-3160.
- Jiang JX, Chen X, Serizawa N, et al. Liver fibrosis and hepatocyte apoptosis are attenuated by GKT137831, a novel NOX4/NOX1 inhibitor in vivo. *Free Radic Biol Med*. 2012;53:289-296.
- Hirano K, Chen WS, Chueng AL, et al. Discovery of GSK2795039, a novel small molecule NADPH oxidase 2 inhibitor. *Antioxid Redox Signal*. 2015;23:358-374.
- Anvari E, Wikstrom P, Walum E, Welsh N. The novel NADPH oxidase 4 inhibitor GLX351322 counteracts glucose intolerance in high-fat diet-treated C57BL/6 mice. *Free Radic Res*. 2015;49:1308-1318.
- Gianni D, Taulet N, Zhang H, et al. A novel and specific NADPH oxidase-1 (Nox1) small-molecule inhibitor blocks the formation of functional invadopodia in human colon cancer cells. *ACS Chem Biol*. 2010;5:981-993.
- Dayal S, Wilson KM, Motto DG, Miller FJ Jr, Chauhan AK, Lentz SR. Hydrogen peroxide promotes aging-related platelet hyperactivation and thrombosis. *Circulation*. 2013;127:1308-1316.
- Stef G, Csiszar A, Ziangmin Z, Ferdinandy P, Ungvari Z, Veress G. Inhibition of NAD(P)H oxidase attenuates aggregation of platelets from high-risk cardiac patients with aspirin resistance. *Pharmacol Rep*. 2007;59:428-436.
- Vara D, Pula G. Reactive oxygen species: physiological roles in the regulation of vascular cells. *Curr Mol Med*. 2014;14:1103-1125.
- Akbar H, Duan X, Saleem S, Davis AK, Zheng Y. RhoA and Rac1 GTPases differentially regulate agonist-receptor mediated reactive oxygen species generation in platelets. *PLoS One*. 2016;11:e0163227.
- Akbar H, Duan X, Piatt R, et al. Small molecule targeting the Rac1-NOX2 interaction prevents collagen-related peptide and thrombin-induced reactive oxygen species generation and platelet activation. *J Thromb Haemost*. 2018;16:2083-2096.
- Jang JY, Min JH, Wang SB, et al. Resveratrol inhibits collagen-induced platelet stimulation through suppressing NADPH oxidase and oxidative inactivation of SH2 domain-containing protein tyrosine phosphatase-2. *Free Radic Biol Med*. 2015;89:842-851.
- Wang SB, Jang JY, Chae YH, et al. Kaempferol suppresses collagen-induced platelet activation by inhibiting NADPH oxidase

- and protecting SHP-2 from oxidative inactivation. *Free Radic Biol Med.* 2015;83:41-53.
29. Gavazzi G, Banfi B, Deffert C, et al. Decreased blood pressure in NOX1-deficient mice. *FEBS Lett.* 2006;580:497-504.
 30. Pollock JD, Williams DA, Gifford MA, et al. Mouse model of X-linked chronic granulomatous disease, an inherited defect in phagocyte superoxide production. *Nat Genet.* 1995;9:202-209.
 31. Bonnard T, Hagemeyer CE. Ferric chloride-induced thrombosis mouse model on carotid artery and mesentery vessel. *J Vis Exp.* 2015:e52838. <https://doi.org/10.3791/52838>
 32. Grover SP, Mackman N. How useful are ferric chloride models of arterial thrombosis? *Platelets.* 2020;31(4):432-438.
 33. Nagy M, van Geffen JP, Stegner D, et al. Comparative analysis of microfluidics thrombus formation in multiple genetically modified mice: link to thrombosis and hemostasis. *Front Cardiovasc Med.* 2019;6:99.
 34. Rochat S, Alberio L. Formaldehyde-fixation of platelets for flow cytometric measurement of phosphatidylserine exposure is feasible. *Cytometry A.* 2015;87:32-36.
 35. Jarvis GE, Raynal N, Langford JP, et al. Identification of a major GpVI-binding locus in human type III collagen. *Blood.* 2008;111:4986-4996.
 36. Vaezzadeh N, Ni R, Kim PY, Weitz JI, Gross PL. Comparison of the effect of coagulation and platelet function impairments on various mouse bleeding models. *Thromb Haemost.* 2014;112:412-418.
 37. Cammisotto V, Carnevale R, Nocella C, et al. Nox2-mediated platelet activation by glycoprotein (GP) VI: effect of rivaroxaban alone and in combination with aspirin. *Biochem Pharmacol.* 2019;163:111-118.
 38. Csanyi G, Cifuentes-Pagano E, Al Ghoulh I, et al. Nox2 B-loop peptide, Nox2ds, specifically inhibits the NADPH oxidase Nox2. *Free Radic Biol Med.* 2011;51:1116-1125.
 39. Youn JY, Gao L, Cai H. The p47phox- and NADPH oxidase organizer 1 (NOXO1)-dependent activation of NADPH oxidase 1 (NOX1) mediates endothelial nitric oxide synthase (eNOS) uncoupling and endothelial dysfunction in a streptozotocin-induced murine model of diabetes. *Diabetologia.* 2012;55:2069-2079.
 40. Bedard K, Krause KH. The NOX family of ROS-generating NADPH oxidases: physiology and pathophysiology. *Physiol Rev.* 2007;87:245-313.
 41. Rezende F, Moll F, Walter M, et al. The NADPH organizers NoxO1 and p47phox are both mediators of diabetes-induced vascular dysfunction in mice. *Redox Biol.* 2018;15:12-21.
 42. Jiang P, Jandrot-Perrus M. New advances in treating thrombotic diseases: GPVI as a platelet drug target. *Drug Discov Today.* 2014;19:1471-1475.
 43. Voors-Pette C, Lebozec K, Dogterom P, et al. Safety and tolerability, pharmacokinetics, and pharmacodynamics of ACT017, an antiplatelet GPVI (Glycoprotein VI) Fab. *Arterioscler Thromb Vasc Biol.* 2019;39:956-964.
 44. Mojica Munoz AK, Jamasbi J, Uhland K, et al. Recombinant GPVI-Fc added to single or dual antiplatelet therapy in vitro prevents plaque-induced platelet thrombus formation. *Thromb Haemost.* 2017;117:1651-1659.
 45. Florian P, Wonerow P, Harder S, Kuczka K, Dubar M, Graff J. Anti-GPVI Fab SAR264565 effectively blocks GPVI function in ex vivo human platelets under arterial shear in a perfusion chamber. *Eur J Clin Pharmacol.* 2017;73:949-956.
 46. Teixeira G, Szyndralewicz C, Molango S, et al. Therapeutic potential of NADPH oxidase 1/4 inhibitors. *Br J Pharmacol.* 2017;174:1647-1669.
 47. Gray SP, Jha JC, Kennedy K, et al. Combined NOX1/4 inhibition with GKT137831 in mice provides dose-dependent reno- and atheroprotection even in established micro- and macrovascular disease. *Diabetologia.* 2017;60:927-937.
 48. Bach RD, Canepa C. Electronic factors influencing the decarboxylation of beta-Keto Acids. A model enzyme study. *J Org Chem.* 1996;61:6346-6353.
 49. Leppanen J, Savolainen J, Nevalainen T, et al. Synthesis and in-vitro/in-vivo evaluation of orally administered entacapone prodrugs. *J Pharm Pharmacol.* 2001;53:1489-1498.
 50. Swan D, Loughran N, Makris M, Thachil J. Management of bleeding and procedures in patients on antiplatelet therapy. *Blood Rev.* 2019;39:100619. <https://doi.org/10.1016/j.blre.2019.100619>
 51. Yasuda H, Matsuo Y, Sato Y, et al. Treatment and prevention of gastrointestinal bleeding in patients receiving antiplatelet therapy. *World J Crit Care Med.* 2015;4(1):40-46.
 52. Mackman N, Bergmeier W, Stouffer GA, Weitz JI. Therapeutic strategies for thrombosis: new targets and approaches. *Nat Rev Drug Discov.* 2020;19:333-352.

SUPPORTING INFORMATION

Additional Supporting Information may be found online in the Supporting Information section.

How to cite this article: Vara D, Tarafdar A, Celikag M, et al. NADPH oxidase 1 is a novel pharmacological target for the development of an antiplatelet drug without bleeding side effects. *The FASEB Journal.* 2020;34:13959–13977. <https://doi.org/10.1096/fj.202001086RRR>